RSC Advances

PAPER

View Article Online
View Journal | View Issue

Cite this: *RSC Adv.*, 2020, **10**, 28376

Highly biodegradable, thermostable eutectogels prepared by gelation of natural deep eutectic solvents using xanthan gum: preparation and characterization

Chaoxi Zeng, *[ab] Haiyang Zhao,[a] Zheng Wan,[a] Qian Xiao,[a] Huiping Xia[a] and Shiyin Guo[ab]

As a possible alternative to hydrogels, eutectogels are formed by gelling natural deep eutectic solvents (NADESs) that may be closer to the intracellular environment than pure water. This study successfully prepared highly biodegradable and thermostable eutectogels based on polysaccharides and NADESs, and studied the possible mechanism of eutectogel formation. The results show that these eutectogels displayed excellent thermostability as both the G' and G'' values remained constant in the temperature range of 60–110 °C, and the weight of the eutectogels remained almost unchanged when held at 80 °C for 10 hours. Similar to the formation of xanthan gum-based hydrogels, water addition and annealing treatment are necessary for the preparation of xanthan gum-based eutectogels. XRD, DSC and FT-IR results show that the existence of xanthan gum affects the original hydrogen bonding network of the NADESs, which further indicate that the hydrogen bond interaction between xanthan gum and NADESs is an important cause of eutectogel formation and changes in gel properties. Rheological results show that the eutectogel is a weak gel with excellent thermostability and structure recovery. As it is more stable than hydrogels and greener than ion gels, the polysaccharide-based eutectogel is expected to be widely used in the fields of food, medicine and materials.

Received 16th April 2020
Accepted 13th July 2020

DOI: 10.1039/d0ra03390a

rsc.li/rsc-advances

Introduction

Natural deep eutectic solvents (NADES), as promising green solvents and unique functional liquid media, have gained popularity in many different areas in recent years.[1–3] NADES are eutectic mixtures formed by mixing two or more common natural products together at specific molar ratios.[4] These natural products are cellular constituents that occur in large amounts in cells, such as sugars, alcohols, amino acids, organic acids and choline derivatives.[5] Due to the nature of such naturally occurring ingredients, NADES are known for several beneficial solvent properties such as biodegradability, sustainability and simplicity of preparation; especially, their biocompatibility means that they are considered as promising alternative solvents for conventional organic solvents and ionic liquids.[6–8] Meanwhile, for the excellent solubility of many non-water-soluble bioactive compounds, NADES are actively applied as prospective extraction media and delivery systems for bioactive compounds in the food and pharmaceutical industries.[9,10]

In order to make better use of a green solvent, it is an effective means to prepare a gel with special properties by gelation. Hydrogels, as a typical type of gel, are extensively applied to the fields of biomedicine and chemistry,[11,12] and ionic gels formed from ionic liquids also have important applications in many fields.[13–15] Similarly, since NADESs can be considered as excellent extraction media and delivery systems for bioactive compounds and enzymes, although recent research is still in its infancy, NADES-based gels are expected to have wide application potential in food and medicine.[16] Besides, from the perspective of cell biology, since NADES is presumed to be a possible third liquid in biological cells other than water and oil,[4,17] and as the gel nature of cytoplasm is increasingly recognized,[18,19] the study of gels based on NADES will help to enhance the understanding of cellular metabolism in biological systems.

Polysaccharides are natural polymers from renewable sources, and have attracted enormous attention due to their peculiar properties such as ready availability, cost-effectiveness, and excellent biocompatibility that make them suitable for various applications.[20] The utilization of these highly biodegradable biopolymers as supporting scaffolds in gels offers an appealing

[a]*Department of Food Science and Technology, College of Food Science and Technology, Hunan Agricultural University, Changsha, China. E-mail: chaoxizeng@hunau.edu.cn*
[b]*Hunan Rapeseed Oil Nutrition Health and Deep Development Engineering Technology Research Center, Hunan Agricultural University, Changsha, China*

way to advance gel biocompatibility.[21,22] Among them, xanthan gum, an anionic microbial polysaccharide produced commercially by bacterial fermentation, is a versatile biopolymer widely used in hydrogel preparation for biomedical and technological applications.[23] Especially, xanthan gum has recently attracted great attention as a biomaterial for the preparation of tissue scaffolds (extracellular matrix) for tissue engineering applications. Although there is already a concept of "eutectogel" based on DES and gels formed by chemically synthesized gelators,[24–27] to the best of our knowledge, there are still only few reports on the formation of polysaccharide-based eutectogels based on NADESs. In particular, the formation mechanism of polysaccharide-based eutectogels remains to be studied.

In this study, highly biodegradable, thermostable eutectogels were successfully prepared by gelation of NADESs by low-cost, biocompatible and biodegradable polysaccharide xanthan gum. Structure and morphology were investigated by polarized optical microscopy (POM) and scanning electron microscopy (SEM), the possible gel mechanism was investigated by Fourier-transform infrared spectroscopy (FT-IR) and X-ray diffraction (XRD), and rheological properties were also studied. The study provides some fundamental information on novel polysaccharide-based eutectogels, which will be beneficial for their wide application in food, agriculture, cosmetics, biomedicine, and other fields.

Results and discussion

Preparation of xanthan gum-based eutectogels

In this study, polysaccharide-based eutectogels were successfully prepared by gelation of NADESs using xanthan gum as a gelator. Considering the possible influence of high viscosity of NADESs on gel preparation, four relatively low-viscosity choline chloride-based NADESs were selected as the test solvents. The hydrogen bonding donors were glycerol, xylitol, sorbitol and citric acid. Results showed that the gelation of these four NADESs occurred when low concentrations (less than 5%) of xanthan gum were used as a universal gelator for NADESs. Fig. 1 shows a schematic illustration of the eutectogel preparation process. Obviously, not only are the NADESs biodegradable and simple to prepare, but their corresponding gels have the characteristics of natural origin and simple preparation. Meanwhile, it is worth noting that the preparation of eutectogels requires consideration of preparation conditions, such as water addition and annealing treatment.

Proper water addition is necessary for the xanthan gum eutectogel formation. Fig. 2 shows the eutectogels formed by

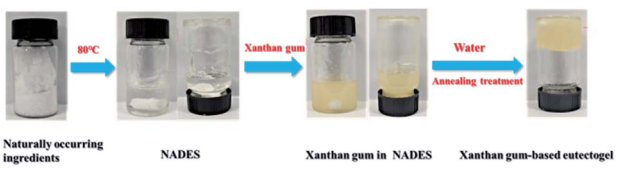

Fig. 1 Schematic diagram of the xanthan gum-based eutectogels preparation process.

Fig. 2 Effects of water addition and different xanthan gum concentrations on the formation of eutectogels.

choline chloride–xylitol in the anhydrous state and that after the addition of 10 wt% water. Results showed that, within the concentration range of 1% to 5% xanthan gum added, gel formation did not happen without the addition of water. However, when a small amount of water was added (10%), even 3% of gelator concentration was sufficient to gelatinize the NADESs. Moreover, except that weak gels formed in the ChCl–Gly possibly due to the cross-linked reaction between glycerol and xanthan gum,[28] no gel formed among these NADESs under anhydrous conditions even if 10% of xanthan gum was added (data not shown). Therefore, we can infer that for other solvents in this study, water molecules are involved in the formation of the eutectogels. The study of Takahashi *et al.* found that water molecules play an important role in the gelation process of xanthan gum hydrogel, and the structural changes of xanthan gum/water system are accompanied by the desorption and adsorption behavior of non-freezing water, which has also been demonstrated in other polysaccharide-based hydrogels.[29,30] Moreover, it is generally believed that the formation of a xanthan gum hydrogel is based on the ordered network structure of xanthan gum formed under annealing conditions with the help of non-freezing water.[31] In xanthan gum hydrogels, the role of water molecules (bound water) is to maintain the ordered conformation of xanthan gum self-assembled aggregates.[30] Therefore, it can be inferred that under normal circumstances, NADES cannot replace water molecules to perform the function of maintaining the ordered conformation of xanthan gum self-assembled aggregates, and thus cannot form gels in such an anhydrous environment.

Meanwhile, it was found that proper annealing treatment is also necessary for xanthan gum eutectogel formation. No gel formation was found in xanthan gum/NADESs mixture containing 10 wt% deionized water that had not been annealed, even when sufficient stirring was provided. However, even if the mixture was heated at 80 °C for only 5 minutes, the eutectogel formed after cooling at room temperature (Fig. 1). This has a clear similarity to the formation properties of xanthan gum-based hydrogels. Xanthan gum, an anionic polysaccharide, consists of a (1-4)-β-D-glucose backbone substituted on every second unit with a charged trisaccharide side chain containing a D-glucuronic acid between two D-mannoses. Xanthan gum exists in a partially ordered conformation in aqueous solution at room temperature. In the ordered structure, the side chains of xanthan gum are associated with the main chain by hydrogen bonds to stabilize the helical structure. As the temperature increases, an "order–disorder" transformation from helix to coil structure happens.[32,33] Intramolecular hydrogen bonds between

the side chains and the main chains are broken, the side chains can move freely, and the molecule undergoes a conformational transformation in solution to afford a flexible disordered conformation. Upon further cooling, the xanthan gum main and side chains re-interact together, forming a more ordered conformation, thereby forming hydrogels.[32] Hence, by comparison with the formation of xanthan gum-based eutectogels and hydrogels, it can be assumed that the xanthan gum molecules in NADESs may exhibit a molecular structure rearrangement similar to that in aqueous solution.

Morphology of xanthan gum-based eutectogels

Microstructures of the xanthan gum-based eutectogels were observed using optical and electron microscopy. Fig. 3 shows POM images of the four xanthan gum-based eutectogels at 10 wt% xanthan gum. As shown in Fig. 3a, in the polarized photomicrograph of the ChCl–Gly eutectogel, a white gauze structure similar to the result of xanthan gum-based hydrogel can be seen, which may be due to the xanthan gum self-assembled aggregate. A similar structure was also observed for the ChCl–Cit eutectogel, where no obvious crystal structure was found (Fig. 3c). However, it is worth noting that crystal structures can be seen for the two sugar alcohol-based eutectogels (Fig. 3b and d), although no crystal structure was observed in the POMs of all four NADESs.

Therefore, by comparing the POM images of the four NADES-based eutectogels, it can be seen that different microstructures displayed in the eutectogels were formed by different NADESs. This may be related to the different hydrogen bonding strengths in different NADESs. NADES is thought to have a supramolecular network structure formed by hydrogen bonding interactions between solvent components.[1] Similarly, the formation of a xanthan gum hydrogel involves maintaining the ordered conformation of xanthan gum by hydrogen bonding. Therefore, in aqueous NADES samples containing xanthan gum, water molecules in NADES may be removed by xanthan gum molecules through hydrogen bonding, resulting in the rearrangement of supramolecular hydrogen bonding networks in NADES. As a result, the eutectic phenomenon weakens and the crystal reappears. Therefore, NADESs with more unstable supramolecular hydrogen bonding network are more susceptible to interference from other foreign components such as xanthan gum.

SEM is an effective method to observe the internal microstructure of various gels. It should be noted that although the actual microstructure of these eutectogels is difficult to accurately observe by electron microscopy because of the need to immerse them in ethanol to remove NADESs, some instructive results can still be obtained. Fig. 4 shows SEM images of the four eutectogels. It was found that different gel microstructures were present in eutectogels with different solvent composition. Although the filamentous structure can be seen in the images of all four eutectogels, the overall structure showed significant differences. As mentioned above, different NADESs have different hydrogen bond network strengths. When the water molecules that maintain the ordered conformation of the xanthan gum self-assembled aggregates were affected by NADESs, the degree of ordering of the xanthan gum conformation decreased. It is possible therefore that the differences in the eutectogel microstructures were due to the different ordered conformations of xanthan gum self-assembled aggregates.

XRD, DSC and FT-IR

XRD, DSC, and FT-IR measurements were made to gain insight into the gel properties of these xanthan gum-based eutectogels. Fig. 5a shows the XRD patterns of anhydrous NADES (ChCl–Xyl), anhydrous NADES (ChCl–Xyl) containing xanthan gum and ChCl–Xyl eutectogel. In the pattern of ChCl–Xyl NADES, only a broad diffraction peak corresponding to the amorphous state of NADES was observed at about 20°. Several sharp peaks were observed in the XRD pattern of the anhydrous ChCl–Xyl containing xanthan gum, which indicated that new crystals formed in the NADES with the participation of xanthan gum molecules. However, for the ChCl–Xyl eutectogel, only a few sharp peaks were seen in the diffraction pattern of the sample. As mentioned above, gels cannot effectively be formed in

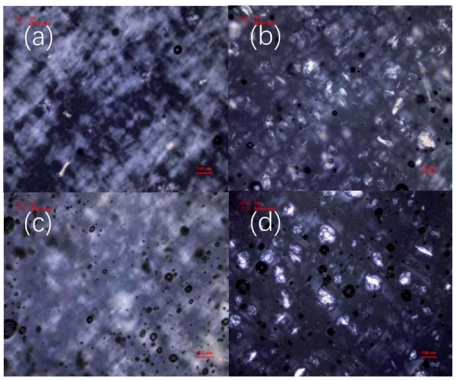

Fig. 3 POM images of xanthan gum-based eutectogels prepared with different NADESs: (a) ChCl–Gly, (b) ChCl–Xyl, (c) ChCl–Cit, (d) ChCl–Sor. Xanthan gum concentration was 10 wt%.

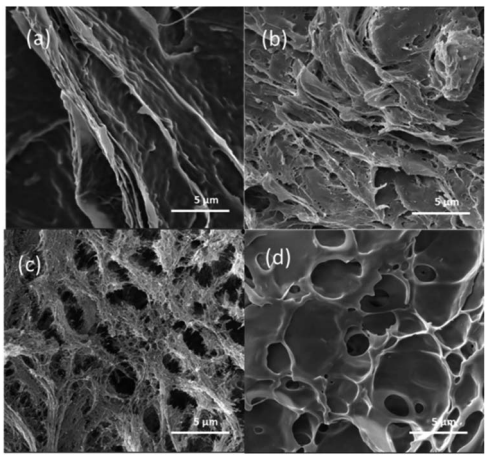

Fig. 4 SEM micrographs of xanthan gum-based eutectogels prepared with different NADESs: (a) ChCl–Gly, (b) ChCl–Cit, (c) ChCl–Xyl, (d) ChCl–Sor. Xanthan gum concentration was 10 wt%.

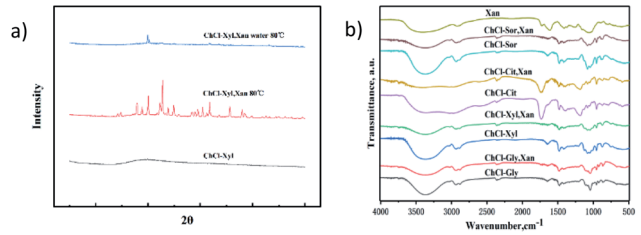

Fig. 5 (a) XRD patterns of anhydrous NADES (ChCl–Xyl), anhydrous NADES (ChCl–Xyl) containing xanthan gum and ChCl–Xyl eutectogel. (b) FT-IR spectra relevant to NADESs and their corresponding eutectogels after water removal.

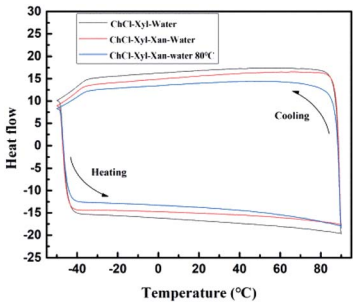

Fig. 6 Differential scanning calorimetry (DSC) of aqueous NADES (ChCl–Xyl–water), aqueous NADES containing xanthan gum (ChCl–Xyl–Xan–water), and the corresponding eutectogel (ChCl–Xyl–Xan–water 80 °C).

NADESs containing xanthan gum without water addition and annealing treatments. It is reported in the literature that the XRD pattern of xanthan gum also shows only a broad diffraction peak around 20°.[34] Therefore, the diffraction pattern of the NADES sample containing xanthan gum may be mainly attributed to the effect of NADES. Marullo *et al.* considered that DESs are fluids with highly ordered and organized structures supported by a complex network of hydrogen bonds.[27] By comparing the XRD patterns of the gels before and after the xanthan gum was added, the results implied a significant change in the ordering of NADES, which may be due to the interference of xanthan gum in the original hydrogen bonding network of the solvent. This also validated the aforementioned POM results, that is, the rearrangement of the hydrogen bonding network in NADESs led to the precipitation of crystals. The addition of water to the NADES samples containing xanthan gum not only facilitates the formation of ordered conformations of xanthan gum self-assembled aggregates, but also reduces the effect of xanthan gum on the hydrogen bonding network in NADES, thus inhibiting the precipitation of crystals.

Fig. 5b shows the FT-IR spectra of xanthan gum, the four NADESs and the corresponding dried xanthan gum-based eutectogels. For xanthan gum, a broad absorption peak at 3399 cm^{-1} indicates the hydrogen bonded –OH groups, and the peaks at 1649 cm^{-1} and 1582 cm^{-1} are attributed to COO- groups. As shown in the figure, compared to the pure NADESs, the O–H stretching peaks at 3368 cm^{-1} of all four tested NADESs after adding xanthan gum have smaller intensities. The above phenomenon suggested that the blending of the xanthan gum with NADESs resulted in variation of the intensities of absorption bands due to hydrogen bonding.[35] This further proved that the existence of xanthan gum affects the original hydrogen bonding network of the NADESs.

To further evaluate the effect of the xanthan gum addition on the NADES supramolecular hydrogen bonding network, we performed DSC tests on three samples with or without xanthan gum. Fig. 6 shows DSC results of the aqueous NADES (ChCl–Xyl–water), aqueous NADES containing xanthan gum (ChCl–Xyl–Xan–water), and the corresponding eutectogel (ChCl–Xyl–Xan–water 80 °C). DSC was used to determine the phase transition temperatures, including melting point (T_m), glass transition temperature (T_g) and crystallization temperature (T_c). As shown in the figure, no melting or freezing points were found in all samples, and the glass transition is the only thermal event detected. This thermal behavior is typical for many DESs in that the glass transition is the only thermal event detected.[36] The glass transition temperatures of the aqueous NADES, aqueous NADES containing xanthan gum, and corresponding eutectogel were exhibited at −49.33, −49.18 and −49.16 °C, respectively. This is similar to the observation of Craveiro *et al.* who reported a decrease in T_g of NADES with water addition due to the destabilization of the supramolecular structure of NADES by water.[36] It can thus be suggested that the addition of xanthan gum during the formation of xanthan gum-based eutectogel does affect the supramolecular hydrogen bond network of the original solvent.

Rheological properties of xanthan gum-based eutectogels

Rheological tests of eutectogels provide important information about their viscoelastic properties. In this study, amplitude sweeps of the four eutectogels were first carried out to determine the linear viscoelastic region (LVR), in which storage modulus (G') was independent of the applied strains (Fig. 7a). It was found that all samples have a higher G' than G'' in the LVR,

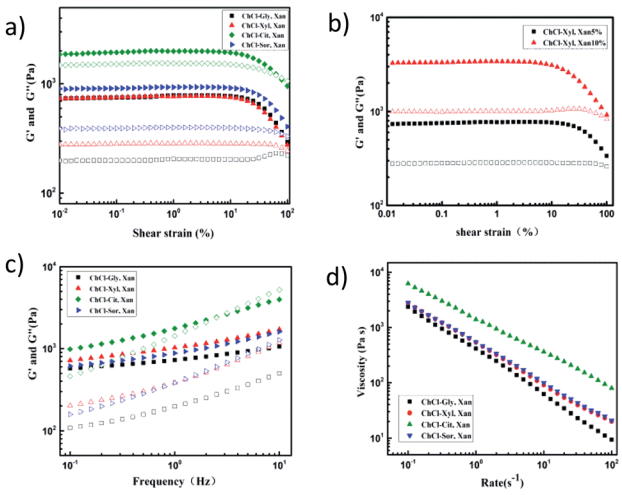

Fig. 7 (a and b) Amplitude sweeps, (c) frequency sweeps, and (d) flow measurements of four xanthan gum-based eutectogels.

revealing that all of the samples displayed gel-like behavior at a xanthan concentration as low as 5 wt%. At the same time, as shown in Fig. 7b, the apparent higher G' of eutectogel with 10% xanthan concentration than that with 5% xanthan concentration indicated that the concentration has a significant influence on the rheological properties of the gels.

Frequency sweep tests offer a convenient way of measuring the deformation properties of gel samples, and allow the classification of samples into strong gels, weak gels, and viscous sols. When modulus value is plotted as a function of frequency, strong gels show frequency independence, while weak gels display frequency-dependent behavior. Fig. 7c shows the frequency dependence of the G' and G'' values of the four eutectogels. According to the frequency sweep results, all the samples exhibited higher values of G' than of G'' throughout the entire range of applied frequency. Therefore, the solid-like viscoelastic properties of these eutectogels can also be proved. Meanwhile, although G' was relatively independent of frequency in the low-frequency region, the slight positive slope of the G' curve and the obvious frequency dependence of G'' both are characteristics for weak gels. In addition, as the frequency increased, G'' gradually approached G', which was a sign of the deformation and re-formation of hydrogen bonding.[37] Therefore, this also proves that the formation of the eutectogel may be based on a rearranged hydrogen bond network formed by xanthan gum molecules and NADES. In addition, compared with ChCl–Gly eutectogel, the G' values of the other three eutectogels changed more obviously with an increase of frequency, especially the ChCl–Cit eutectogel. As mentioned above, this difference may be mainly related to the different hydrogen bond network strengths within these four solvents.

Eutectogel samples were also characterized with flow measurements by subjecting them to increasing shear rates. The viscosity curves are shown in Fig. 7d. All samples behaved as non-Newtonian fluids since the viscosity depended on the shear rate values and showed a strong shear-thinning behavior. Fig. 8a shows the thermo-responsive changes of G' and G'' of the four NADES-based eutectogels. As shown, the dominant elastic structure of the eutectogel samples was retained throughout the studied temperature range (illustrated by $G' > G''$); thus they can be considered thermostable. Especially for ChCl–Gly-based eutectogel, the sample displayed good thermostability as both the G' and G'' values remained constant in the temperature range of 60–110 °C. These results are in agreement with

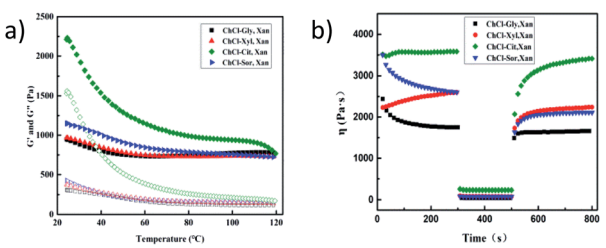

Fig. 8 (a) Temperature sweeps and (b) 3-ITT for structure recovery of four xanthan gum-based eutectogels.

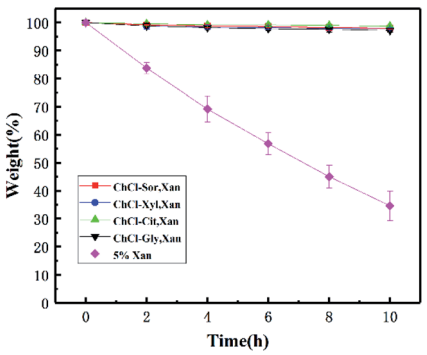

Fig. 9 Weight-holding capacity of four xanthan gum-based eutectogels and the corresponding hydrogel ($n = 3$). Bars indicate standard deviation.

previous data by Liu *et al.* who observed a similar behavior with xanthan gum hydrogel.[38] For the other three gels, it can be clearly observed that the G' and G'' values decreased correspondingly with increasing temperature in the temperature range below 50 °C.

In addition, time-dependent fluid behavior was also studied to gain insights into the thixotropy and structure recovery properties of these NADES-based eutectogels. The structure recovery properties were evaluated by a specific rheological test which is known as the three-interval time test (3-ITT). In the test, the viscosity changes were followed as a function of time under alternative constant shear rates (0.1, 10, and 0.1 s^{-1}). The structure recovery was calculated for each sample by taking the viscosity value at the end of interval 1 as 100% and comparing it with the peak viscosity value in interval 3. As shown in the Fig. 8b, the percentage recovery for all samples exceeded 80%, indicating good structure recovery.

Weight-holding capacity of xanthan gum-based eutectogels

It is well known that hydrogels have a significant disadvantage in that the properties of hydrogels change due to the volatilization of water during gel preservation, which limits their application. In contrast, NADESs are reported to have a strong ability to bind water. Therefore, we also evaluated and compared the weight-holding capacity of two xanthan gum-based gels under accelerated dehydration conditions. As shown in Fig. 9, the gel weight changes of the four eutectogels and the corresponding xanthan gum hydrogel held at 80 °C for 10 hours are compared. The results showed that although the hydrogel lost more than 60% of its weight during the 10 hour storage, the weight of the eutectogels remained almost unchanged. The advantage of excellent weight-holding capacity will be beneficial to the application of the eutectogels in many fields.

Experimental

Materials

Commercially available xanthan gum from *Xanthomonas campestris* ($C_{35}H_{49}O_{29}$, M_w = 600 kDa, USP grade, 95–99%, xanthan powders contain a moisture of *ca.* 12% and an ash of 5.5–13%

cps), xylitol (purity 98%), D-sorbitol (purity ≥98%) and citric acid (purity ≥99.5%) were purchased from Aladdin Ltd (Shanghai, China) and used as received. Glycerol and choline chloride were purchased from Sinopharm Chemical Reagent Co. Ltd (Beijing, China) and used as received.

Preparation of NADESs and xanthan gum-based eutectogels

NADES samples were prepared according to the procedure described in our previous works. All NADES, namely choline chloride–xylitol (ChCl–Xyl, 1 : 1), choline chloride–glycerol (ChCl–Gly, 1 : 2), choline chloride–sorbitol (ChCl–Sor, 1 : 1), and choline chloride–citric acid (ChCl–Cit, 1 : 1), were prepared by mixing choline chloride and a hydrogen bond donor (glycerol, xylitol, sorbitol or citric acid) at certain molar ratios. The resulting mixture was placed in a screw-capped vial with a stirring bar. Then, the mixture was heated with agitation at 80 °C for more than 30 minutes until a clear liquid was obtained.

Eutectogels were prepared by weighing into a screw-capped sample vial suitable amounts of NADES and xanthan gum, and stirring at room temperature until completely dissolved. After 10 wt% deionized water was added to the mixture, the sample vial was heated in a water bath at 80 °C for another 5 minutes. Then, the vial was left to cool at room temperature to form eutectogels.

Characterization

Morphology of xanthan gum-based eutectogels

Morphologies of the xanthan gum-based eutectogels were observed under white and polarized lights using an Olympus microscope (BX53M; Olympus, Shinjuku, Japan). The prepared eutectogel samples were when hot dropped on a glass slide and cooled to form gels, and then examined under white and polarized lights. SEM images were acquired using an FEI Quanta FEG 250 scanning electron microscope with an operating voltage of 30 kV. Samples were prepared by suspended the eutectogels in ethanol in a vial for 5 days, and the anhydrous ethanol was changed every 24 hours until the NADES was completely replaced. The soaked samples were quickly frozen and converted to xerogels by freeze drying for several hours. The samples were then introduced into the SEM machine and sputter-coated with a thin film of gold prior to imaging.

FT-IR spectra

FT-IR spectra of samples were recorded with an FT-IR spectrometer (Shimadzu IRAffinity-1; Shimadzu Corp, Kyoto, Japan). Various eutectogel samples were freeze-dried and milled with KBr powder. The resulting spectra were analyzed using OPUS software (Bruker Corporation) in the range of 400–4000 cm^{-1} with a resolution of 2 cm^{-1}. The background scan was performed before each sample measurement. All spectra were averaged from at least duplicate measurements with 32 scans before baseline correction and smoothing.

X-ray diffraction

XRD profiles for samples were obtained using an X-ray diffractometer (MiniFlex-600, Rigaku Corporation, Japan) at 25 °C. The scanning angle was from 5° to 80° with a scanning speed of 10° min^{-1} at 40 kV voltage and 15 mA current.

DSC

To assess the thermal behavior of the NADES, calorimetric experiments were carried out with a DSC Q2000 from TA Instruments Inc. (Tzero™ DSC Technology) operating in the Heat Flow T4P option. Measurements were performed under dry high-purity helium, at a flow rate of 50 mL min^{-1}. Less than 5 mg of each sample was encapsulated in Tzero aluminum pans.

Rheology measurements

The rheological measurements were conducted by using a Kinexus Pro rotational rheometer (Malvern Instruments, UK) equipped with a stainless-steel cone and plate geometry (diameter 40 mm, gap set to 1 mm). Typical rheology experiments used 1 Hz as the initial value to test the gels in an amplitude sweep. A sweep of strain from 0.05 to 100% was selected for the tests. The frequency sweep was carried out to measure shear storage modulus (G') and loss modulus (G'') as a function of angular frequency over the range of 1–10 Hz. To determine the viscosity, dynamic flow sweep was conducted with a shear rate from 0.1 to 100 s^{-1}. A temperature sweep with a cooling and heating rate of 1 °C min^{-1} at a constant angular frequency of 1 rad s^{-1} and fixed strain of 1% was carried out from 80 °C to 20 °C and subsequently from 20 °C to 80 °C, respectively. All the experiments were carried out at 25 °C and all samples were equilibrated for 2 min before measurements.

Conclusions

In the application of many bio-related materials, biodegradability and stability are the key indicators to be considered. NADESs are eutectic mixtures formed by mixing two or more cellular constituents that occur in large amounts in cells together at specific molar ratios; thus they are known for several beneficial solvent properties such as biodegradability, sustainability and biocompatibility. In this study, biodegradable polysaccharide-based eutectogels were prepared using xanthan gum as an effective gelator for NADESs. The results show that these eutectogels displayed excellent thermostability as both the G' and G'' values remained constant in the temperature range of 60–80 °C, and the weight of the eutectogels remained almost unchanged when held at 80 °C for 10 hours.

Meanwhile, it was found that the successful preparation of eutectogels requires the addition of an appropriate amount of water and heating–cooling treatment. By comparing with the formation mechanism of hydrogels, it can be inferred that the formation mechanism of xanthan gum-based eutectogel is similar to that of xanthan gum-based hydrogel. The difference is the rearrangement of NADESs' hydrogen bond network by xanthan gum and the ordered conformations of xanthan gum

self-assembled aggregates in NADESs affected by the hydrogen bond network of NADESs.

Since the NADES is a kind of controllable solvent (based on the combination of different components, various solvents can be formed), it is beneficial for obtaining various eutectogels with different gel properties. Therefore, based on the natural source characteristics of its components, as a new type of gel with more advantages than traditional hydrogels and ionic gels, this biodegradable and thermostable eutectogel is expected to show more application prospects.

Conflicts of interest

There are no conflicts to declare.

Acknowledgements

This work was supported by the National Natural Science Foundation of China (grant number 31701580) and the Natural Science Foundation of Hunan Province (grant number 2019JJ50229).

References

1 A. Paiva, R. Craveiro, I. Aroso, M. Martins, R. L. Reis and A. R. C. Duarte, *ACS Sustainable Chem. Eng.*, 2014, **2**, 1063–1071.
2 I. Zahrina, M. Nasikin, E. Krisanti and K. Mulia, *Food Chem.*, 2018, **240**, 490–495.
3 T.-X. Yang, L.-Q. Zhao, J. Wang, G.-L. Song, H.-M. Liu, H. Cheng and Z. Yang, *ACS Sustainable Chem. Eng.*, 2017, **5**, 5713–5722.
4 Y. H. Choi, J. van Spronsen, Y. Dai, M. Verberne, F. Hollmann, I. W. Arends, G. J. Witkamp and R. Verpoorte, *Plant Physiol.*, 2011, **156**, 1701–1705.
5 Y. Dai, J. van Spronsen, G. J. Witkamp, R. Verpoorte and Y. H. Choi, *Anal. Chim. Acta*, 2013, **766**, 61–68.
6 R. Martínez, L. Berbegal, G. Guillena and D. J. Ramón, *Green Chem.*, 2016, **18**, 1724–1730.
7 C. Wu, H.-J. Xiao, S.-W. Wang, M.-S. Tang, Z.-L. Tang, W. Xia, W.-F. Li, Z. Cao and W.-M. He, *ACS Sustainable Chem. Eng.*, 2019, **7**, 2169–2175.
8 Á. Mourelle-Insua, I. Lavandera and V. Gotor-Fernández, *Green Chem.*, 2019, **21**, 2946–2951.
9 D. C. Murador, L. M. de Souza Mesquita, N. Vannuchi, A. R. C. Braga and V. V. de Rosso, *Curr. Opin. Food Sci.*, 2019, **26**, 25–34.
10 W. C. Huang, D. Zhao, N. Guo, C. Xue and X. Mao, *J. Agric. Food Chem.*, 2018, **66**, 11897–11901.
11 C. Yang and Z. Suo, *Nat. Rev. Mater.*, 2018, **3**, 125–142.
12 E. Caló and V. V. Khutoryanskiy, *Eur. Polym. J.*, 2015, **65**, 252–267.
13 S. Marullo, C. Rizzo, N. T. Dintcheva, F. Giannici and F. D'Anna, *J. Colloid Interface Sci.*, 2018, **517**, 182–193.
14 K. M. Bothwell, F. Lorenzini, E. Mathers, P. C. Marr and A. C. Marr, *ACS Sustainable Chem. Eng.*, 2018, **7**, 2686–2690.
15 I. Osada, H. de Vries, B. Scrosati and S. Passerini, *Angew. Chem., Int. Ed.*, 2016, **55**, 500–513.
16 C. Mukesh, R. Gupta, D. N. Srivastava, S. K. Nataraj and K. Prasad, *RSC Adv.*, 2016, **6**, 28586–28592.
17 A. A. Hyman and K. Simons, *Science*, 2012, **337**, 1047–1049.
18 B. R. Parry, I. V. Surovtsev, M. T. Cabeen, C. S. O'Hern, E. R. Dufresne and C. Jacobs-Wagner, *Cell*, 2014, **156**, 183–194.
19 R. Grygorczyk, F. Boudreault, A. Platonova and S. N. Orlov, *Pflügers Arch.*, 2015, **467**, 475–487.
20 Y. Hu, Y. Li and F. J. Xu, *Acc. Chem. Res.*, 2017, **50**, 281–292.
21 J. Radhakrishnan, A. Subramanian, U. M. Krishnan and S. Sethuraman, *Biomacromolecules*, 2017, **18**, 1–26.
22 A. Kirschning, N. Dibbert and G. Drager, *Chemistry*, 2018, **24**, 1231–1240.
23 D. F. S. Petri, *J. Appl. Polym. Sci.*, 2015, **132**, 23.
24 B. Joos, T. Vranken, W. Marchal, M. Safari, M. K. Van Bael and A. T. Hardy, *Chem. Mater.*, 2018, **30**, 655–662.
25 J. Ruiz-Olles, P. Slavik, N. K. Whitelaw and D. K. Smith, *Angew. Chem., Int. Ed.*, 2019, **58**, 4173–4178.
26 H. Qin, R. E. Owyeung, S. R. Sonkusale and M. J. Panzer, *J. Mater. Chem. C*, 2019, **7**, 601–608.
27 S. Marullo, A. Meli, F. Giannici and F. D'Anna, *ACS Sustainable Chem. Eng.*, 2018, **6**, 12598–12602.
28 D. Bilanovic, J. Starosvetsky and R. H. Armon, *Food Hydrocolloids*, 2015, **44**, 129–135.
29 M. Takahashi, T. Hatakeyama and H. Hatakeyama, *Carbohydr. Polym.*, 2000, **41**, 91–95.
30 H. Yoshida, T. Hatakeyama and H. Hatakeyama, *J. Therm. Anal. Calorim.*, 1993, **40**, 483–489.
31 T. H. Francis and X. Quinn, *Polymer*, 1994, **35**, 1248–1252.
32 M. Iijima, M. Shinozaki, T. Hatakeyama, M. Takahashi and H. Hatakeyama, *Carbohydr. Polym.*, 2007, **68**, 701–707.
33 E. R. Morris, *Food Hydrocolloids*, 2019, **86**, 18–25.
34 H. Izawa and J.-i. Kadokawa, *J. Mater. Chem.*, 2010, **20**, 5235–5241.
35 R. Balasubramanian, S. S. Kim and J. Lee, *Int. J. Biol. Macromol.*, 2018, **118**, 561–568.
36 R. Craveiro, I. Aroso, V. Flammia, T. Carvalho, M. T. Viciosa, M. Dionísio, S. Barreiros, R. L. Reis, A. R. C. Duarte and A. Paiva, *J. Mol. Liq.*, 2016, **215**, 534–540.
37 Y. Yue, J. Han, G. Han, A. D. French, Y. Qi and Q. Wu, *Carbohydr. Polym.*, 2016, **147**, 155–164.
38 Z. Liu and P. Yao, *Carbohydr. Polym.*, 2015, **132**, 490–498.

